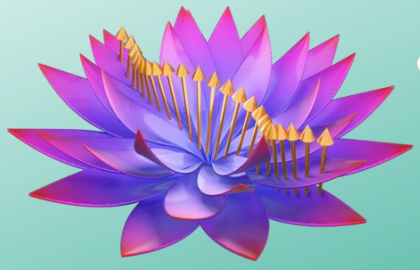

NIMFEIA

# Deliverable D2.5

## Report on preliminary electrical characterisation using individually contacted magnetic tunnel junctions

| | |
|---|---|
| Project Number | 101070290 |
| Project name | Nonlinear Magnons for Reservoir Computing in Reciprocal Space |
| Project acronym | NIMFEIA |
| Work Package | WP2 Laboratory-scale experiments |
| Type | Report |
| Dissemination Level | Public |
| Lead Beneficiary | INL |
| Due date of delivery | Month 24 – September 2024 |

Disclaimer:

The NIMFEIA project has received funding by the European Union's Research and Innovation Programme Horizon Europe under grant agreement No 101070290. However, views and opinions expressed in this document are those of the authors only and do not necessarily reflect those of the European Union. The European Union cannot be held responsible for them.

# 1 Introduction

This document acts as an overview of the efforts made to characterise individual Magnetic Tunnel Junctions (MTJs) which were fabricated at INL in the context of reservoir computing in reciprocal space, related to Task 2.6. These devices are similar to those characterised optically in Task 2.1 and can be compared to the simulation outputs gathered in WP3. The output of this characterisation activity acts as an input for WP4 (Materials and device fabrication) and WP5 (Electrical readout for wafer-scale integration).

The goal of the characterisation is to identify the different mechanisms to achieve electrical excitation and read-out in vortex-based MTJs, as well as exploring the different modes present as a function of material and geometry.

# 2 Device fabrication and materials

The devices under investigation are magnetic tunnel junctions, consisting of a complex set of magnetic layers. An example of such a magnetic stack is 6 IrMn / 2 $CoFe_{30}$ / 0.7 Ru / 2.6 $CoFe_{40}B_{20}$ / MgO [8 ohm um2] / 2.0 $CoFe_{40}B_{20}$ / 0.21 Ta / 7 NiFe, where the CoFeB/Ta/NiFe composite is considered to be the free layer, whose magnetisation can vary. The free layer will have a magnetic vortex as the ground state for diameters d > 200 nm, where the in-plane magnetisation will form increasingly small circular loops, whose sense of rotation will define the vortex core chirality, and a central out of plane vortex core, whose direction will define the polarity of the vortex. The CoFeB is required for correct crystallisation of the MgO layer, and the NiFe layer is chosen as a soft magnetic material. The Ta dusting layer stops interaction in crystal texture between the NiFe and CoFeB layer. The CoFe/Ru/CoFeB is a synthetic antiferromagnet (SAF) with the upper layer acting as the fixed layer, whose magnetisation remains fixed.

## 2.1.1 Nanofabrication process

A variety of magnetic stacks were nanofabricated into magnetic tunnel junctions (MTJ) devices using the INL cleanroom facilities. The flow process of conventional magnetic tunnel junction process is shown in Figure 1 and involves the deposition, pillar definition and electrical access steps required for a magnetic tunnel junction along with an additional metal line which is fabricated into a field line strip. The field line is an important element to the NIMFEIA devices as it allows the separation of the excitation and readout mechanisms, which allows higher power signal excitation.

This project has received funding from the EU Research and Innovation Programme Horizon Europe under grant agreement No 101070290.

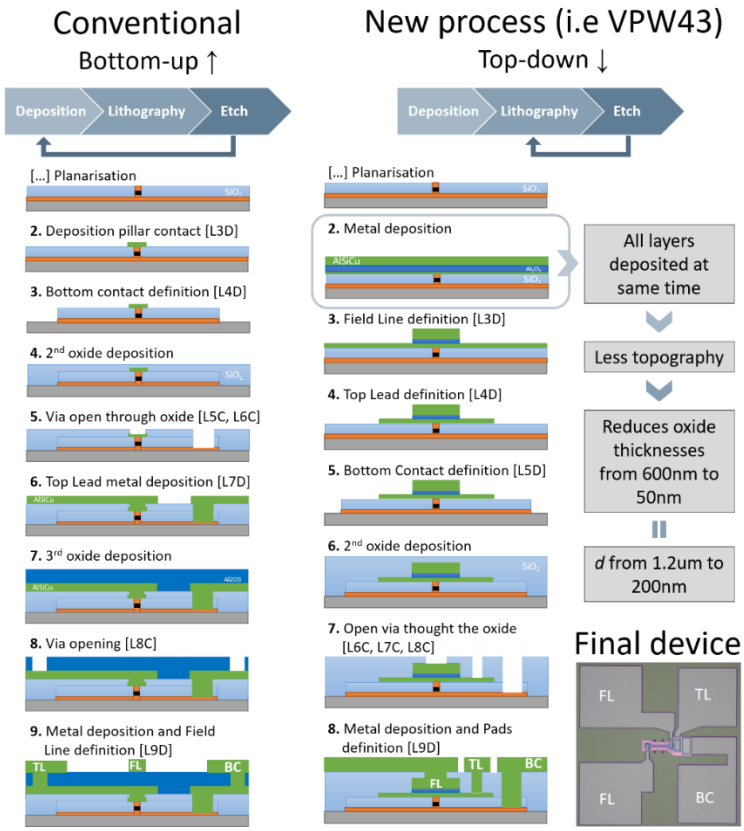


*Figure 1 – comparison of the conventional and new field line process*

A cross-sectional transmission electron microscope (TEM) of the two different processes are presented in Figure 2. The conventional process clearly has a much larger separation between the field line and the MTJ pillar. For the new field line process the top contact thickness and separating oxide can be significantly reduced due to the simultaneous top contact and field line deposition which leads to an increase in the efficiency of the field line. For the conventional process the efficiency value was found to be **0.66 Oe/m** and the new field line process was found to be **1.8 Oe/m**.

This project has received funding from the EU Research and Innovation Programme Horizon Europe under grant agreement No 101070290.

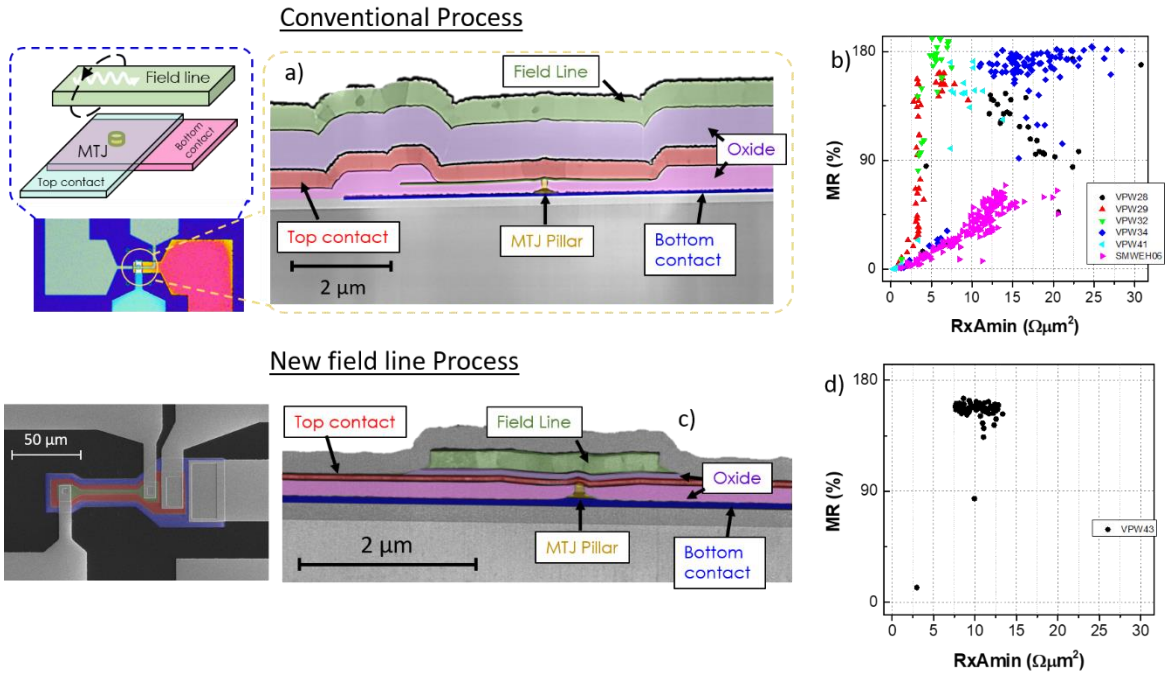


*Figure 2 – a), c) TEM comparison and b), d) resistance area versus TMR of the conventional and new field line process respectively*

Whilst the conventional process allowed the deposition of high quality MTJ devices, the overall yield was problematic due to the topography of the deposition of multiple layers which could often lead to shorts in the metal layers. These shorts are characterised by a lower than expected Resistance x Area (RA) product, as can be seen for a variety of devices fabricated with this process in Figure 2 b).

To address this issue with overall device yield, a new fabrication process was adopted with the simultaneous deposition of the top contact and field line, which can be seen in Figure 1. This process has led to significant reduction in overall dispersion of the static properties of the MTJ devices, as shown in Figure 2 d), where there is a tight bunching of many different nominally identical devices.

### 2.1.2 Magnetic tunnel junction stacks

An overview of the different MTJ devices which were fabricated by INL and characterised both at INL and shared with other NIMFEIA partners can be seen in Table 1.

| Internal reference | Stack details (thickness in nanometres) | Description |
|---|---|---|
| VPW42 | 6 IrMn / 2 $CoFe_{30}$ / 0.825 Ru / 2.6 $CoFe_{40}B_{20}$ / MgO [8.2 Ohm um2] / 1.25 $CoFe_{40}B_{20}$ / 0.21 Ta / 2.5 CoFeSiB | CoFeSiB 3nm free layer⁺ |
| VPW32 | 6 IrMn / 2 CoFe30 / 0.825 Ru / 2.6 CoFe40B20 / MgO [8 Ohm um2] / 2.0 CoFe40B20 / 0.21 Ta / 9 CoFeSiB | CoFeSiB 3nm free layer⁺ |
| VPW46 | 6 IrMn / 2 $CoFe_{30}$ / 0.825 Ru / 2.6 $CoFe_{40}B_{20}$ / MgO [8 Ohm um2] / 2.0 $CoFe_{40}B_{20}$ / 0.21 Ta / 20 CoFeSiB | CoFeSiB 3nm free layer⁺ |
| VPW32 | 6 IrMn / 2 $CoFe_{30}$ / 0.825 Ru / 2.6 $CoFe_{40}B_{20}$ / MgO [8 Ohm um2] / 2.0 $CoFe_{40}B_{20}$ / 0.21 Ta / 40 CoFeSiB | CoFeSiB nm free layer⁺ |
| VPW50 | 6 IrMn / 2 $CoFe_{30}$ / 0.825 Ru / 2.6 $CoFe_{40}B_{20}$ / MgO [6 Ohm um2] / 2.0 $CoFe_{40}B_{20}$ / 0.21 Ta / 80 CoFeSiB | CoFeSiB 80nm free layer⁺ |
| VPW43 | 6 IrMn / 2 $CoFe_{30}$ / 0.7 Ru / 2.6 $CoFe_{40}B_{20}$ / MgO [8 ohm um2] / 2.0 $CoFe_{40}B_{20}$ / 0.21 Ta / 7 NiFe | Standard NiFe free layer* |

⁺ - conventional process,
* - new process

*Table 1 – overview of devices fabricated in the context of the NIMFEIA project*

This project has received funding from the EU Research and Innovation Programme Horizon Europe under grant agreement No 101070290.

The devices fabricated in Table 1 are either using a standard NiFe free layer (which has been previously demonstrated as a multifunctional and versatile magnetic vortex-based MTJ stack) or the more exploratory CoFeSiB, which has been selected as it demonstrates the interesting property of being amorphous even after standard MTJ annealing conditions (330°C, 1T, 1 hour). This amorphous property is essential due to the impact of local pinning sites generated by granular defects in the magnetic free layer. Magnetic vortices are extremely sensitive to these defects due to the relatively small size of the magnetic vortex core (around 20 nm), which can easily become trapped. Further discussion of this and the role it plays in the reservoirs will be discussed in D4.4.

# 3 Electrical characterisation of individual magnetic tunnel junctions with magnetic vortex as ground state

### 3.1.1 Transduction mechanisms comparison

In MTJs the variation in the magnetisation of the free layer can be converted into an electrical signal via the tunnelling magnetoresistance (TMR) effect. There are two main transduction mechanisms present in MTJs which allow for the exploration of magnetisation dynamics, namely:

1. **dc to rf** – the application of a dc current can be used to convert any high frequency resistance oscillations into a radio-frequency voltage, which can be measured by a spectrum analyser. The high frequency resistance oscillations can induced by pumping with an external signal or simply by thermal relaxation.
2. **rf to dc** – applying a rf current at the frequency of resonance of one of the modes induces an high frequency resistance response. The mixing of the current and resistance (of similar frequencies) induces a voltage with a dc component which can be measured using a simple voltmeter, also known as the spin-diode approach.

To better understand the different measurement techniques, in Figure 3 a schematic of the two are presented and measurements of the two techniques using the same MTJ of 1 micron using the VPW43 stack. For the dc to rf, a dc current is applied and a spectrum analyser is used to measure the resultant dynamics. In this case a specific mode is driven by the application of an rf current to the field line antenna located above the MTJ, $I_{rf}^{FL}$. The field line antenna results in a time varying resistance, however this can only be measured as a voltage by the application of the dc current.

### 3.1.2 Three magnon scattering

In Figure 3 b) the rf power measured at the MTJ is plotted as a function of the measurement frequency. A peak at 3.8 GHz is visible corresponding to the excitation frequency in the field line. This peak will be made up of components of the MTJ oscillating at 3.8 GHz as well as some capictively coupled leakage signal from the field line present in the MTJ. Additionally, there are two peaks visible at frequencies around 1.1 and 2.8 GHz which are not at the frequency of the incoming rf signal and can therefore only be associated with dynamics inside the MTJ itself, for example 3 magnon scattering. The output power is measured as a function of the power applied to the field line at 3.8 GHz, i.e. $P_{rf}^{FL}$ and shown in Figure 3 c). At low powers there doesn't seem to be a significant response. As the power is increased, i.e. 7.5 dBm, a peak at the gyrotropic frequency (i.e. ~200 MHz) emerges, due to the coupling between the higher order modes and

This project has received funding from the EU Research and Innovation Programme Horizon Europe under grant agreement No 101070290.

the fundamental mode. As the power increases different modes are visible due to the extremely non-linear nature of the system.

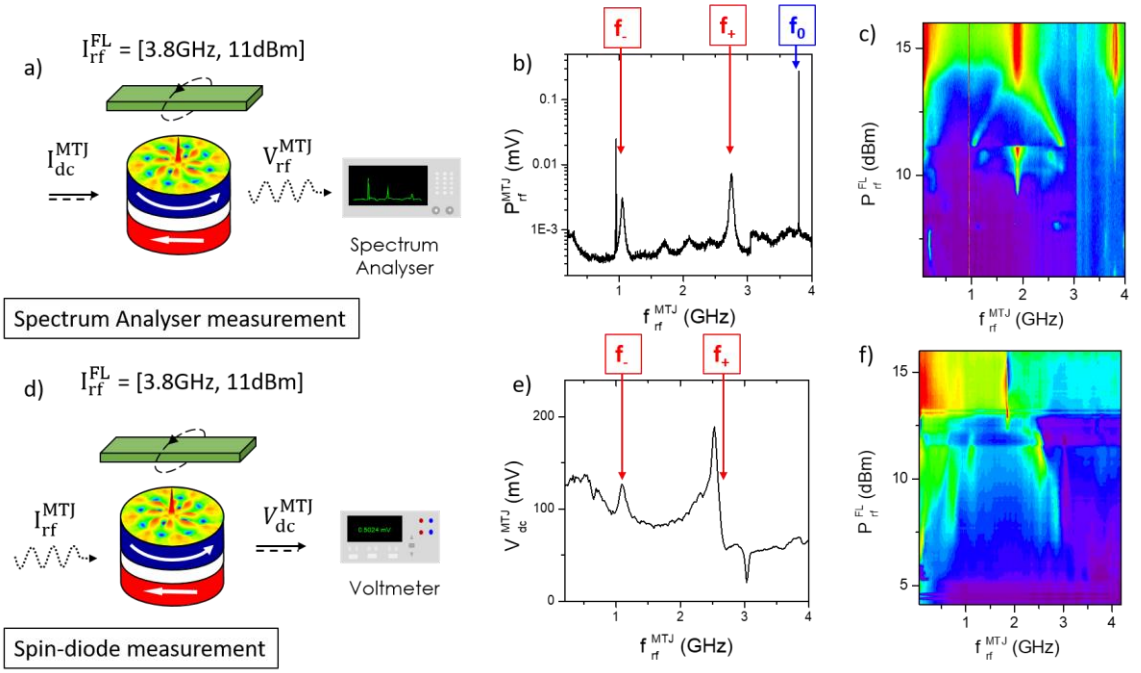


*Figure 3 – overview of different electrical measurement techniques for a) dc to rf and d) rf to dc.*

In Figure 3 d) the rf to dc measurement technique is schematically demonstrated. In this case two rf signals are applied, firstly the same 3.8 GHz signal is applied to the MTJ via the field line, but there is an additional rf current which is applied directly to the MTJ itself, the frequency of which is swept. If the MTJ has resistive dynamics at the frequency of the rf signal applied to the MTJ then there will be a resultant peak in dc voltage. It is important to note that it is assumed (and has been tested by reducing the rf power in the MTJ) that the dynamics are mostly induced by the rf signal in the field line which is significantly larger than the signal in the MTJ. The rf signal in the MTJ is there for measurement and is not believed to induce significant dynamical behaviour itself, although this needs further testing to be certain.

Similar peaks in frequency around 1.1 and 2.8 GHz can be observed, suggesting that both measurement techniques can be used to observe the 3 magnon scattering. The power dependence is not identical to the dc to rf method, probably due to the influence of the dc or rf current on the dynamical behaviour, however, there are qualitatively similar trends observed. These include the low power (~7.5 dBm) excitation of the gyrotropic mode, which then seems to become a split excitation showing two peaks at f- and f+, before becoming a single peak at f0/2.

### 3.1.3 Higher order sidebands

In addition to the 3 magnon scattering, which is the central scattering mechanism for the proposed reservoir computing scheme in the NIMFEIA project, preliminary results have shown a strong coupling between the higher order modes and the gyrotropic mode. An example of this can be seen in Figure 4, where a radio frequency signal is driven across an adjacent field line with a frequency of

This project has received funding from the EU Research and Innovation Programme Horizon Europe under grant agreement No 101070290.

$f_{source}$ = 3.3 GHz and the resultant dynamics are measured with a spectrum analyser. As well an expected peak at the excitation frequency due to a leakage of the signal between the field line and the MTJ, additional sidebands located at $f_{source} \pm f_{gyro}$, $\pm 2f_{gyro}$……, in addition to a peak at the gyrotropic frequency itself. This effect is believed to be related to the strong coupling between the higher order spin wave modes and the gyrotropic mode [1], which when sufficiently strong, results in an orbital motion of the vortex core, which in turn modifies the excited spin wave modes, whose mode profile depends strongly on the vortex core position.

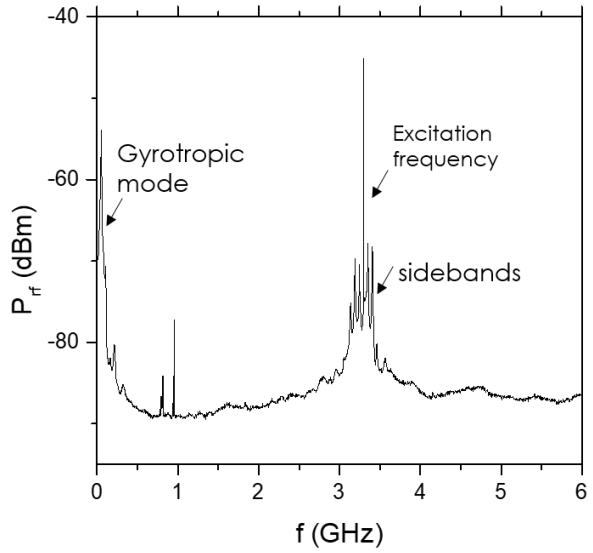


*Figure 4 – measured spectra of an MTJ device when the higher order mode is excited, demonstrating strong coupling with the gyrotropic mode.*

### 3.1.4 Reservoir optimisation

One key question which needs to be addressed for the vortex-based reservoirs is "*what makes a good reservoir?*". Whilst this is a complicated question, and will depend on support from WP6, one clear requirement in the short term is a surplus of available modes in which to scatter into. Effort has therefore been made in terms of analysing the devices shown in Table 1 in terms o f reservoir performance. The fundamental mode of vortex-based MTJs is the gyrotropic mode, which corresponds to a circular orbital motion of the magnetic vortex core. The frequency of the gyrotropic mode can be controlled by modification of the geometry. The variation the frequency of individual MTJs by modification of the geometry is of significant importance when designing the reservoir. The thickness dependence of the fundamental gyrotropic mode is shown in Figure 5 with the corresponding Thiele model fit from

$$k_{ms} = \frac{\left(\frac{10}{9}\right)\mu_0 M_{sat}^2 t^2}{r}, G = \frac{2\pi t M_{sat}}{\gamma}, f = \frac{k_{ms}}{2\pi G}$$

Where $M_{sat}$ is the saturation magnetisation, t is the thickness, r is the device radius, γ is the gyromagnetic ratio. The experimental data can be seen to strongly diverge form the model for thicknesses above ~30 nm. The phenomenon has been discussed via micromagnetic simulations previously and is believed to be related to the fact that the exchange length in such systems is ~10

This project has received funding from the EU Research and Innovation Programme Horizon Europe under grant agreement No 101070290.

nm, and as the film thickness becomes multiple values of the exchange length, the vortex core can no longer be considered two dimensional and high order gyrotropic modes needs to be considered [2].

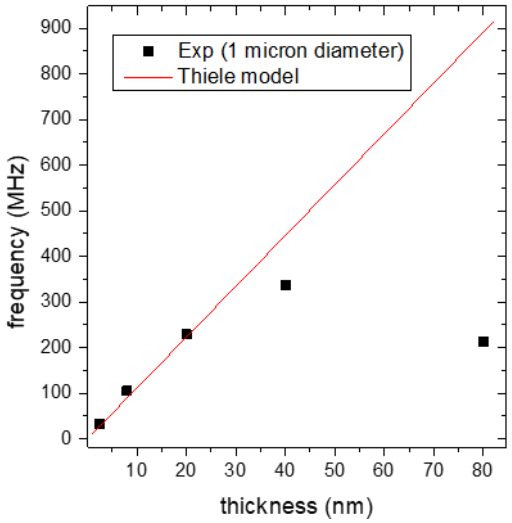


*Figure 5 – frequency of the gyrotropic mode of the vortex-based MTJs as a function of the thickness (for a 1 micron diameter).*

In order to understand better the thickness dependence, in Figure 6 the spin diode measurements were performed for three different devices of diameter 600 nm and free layer thickness 20, 40 and 80 nm CoFeSiB. For the 20nm thick free layer, the vortex can still be considered two dimensional and the modes which are present are the fundamental gyrotropic mode around 440 MHz, with two higher order modes visible between 4-5 GHz corresponding to the first order azimuthal spin wave modes and additional modes visible around 6.5 and 8.5 GHz, where higher order modes are visible corresponding to modes with larger radial and azimuthal indices i.e. n and m, respectively.

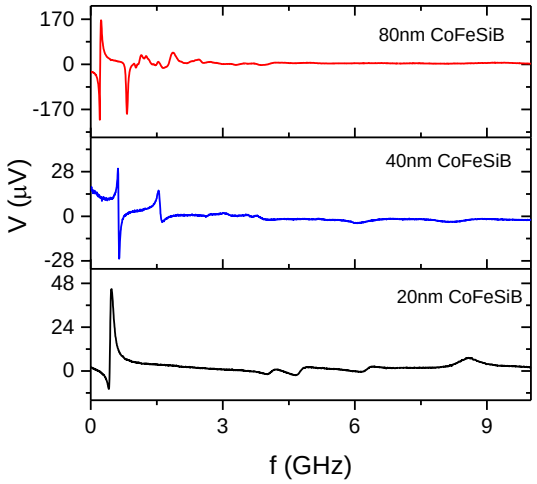


*Figure 6 – spin diode voltage as a function of the applied frequency for a Prf = -20dBm for a 600 nm diameter device for devices with free layer thickness 20, 40 and 80 nm CoFeSiB*

The 80 nm free layer shown in Figure 6 is an example of a three dimensional vortex, where a considerable amount of lower frequency modes are visible, corresponding to the higher order

This project has received funding from the EU Research and Innovation Programme Horizon Europe under grant agreement No 101070290.

gyrotropic modes which arise due to the formation of nodes within the vortex core along the z-direction [2]. The 40 nm thick CoFeSiB free layer is in the transition region between two and three dimensional, with one higher order gyrotropic mode visible as well as the higher order spin wave modes.

### 3.1.5 Magnetic field dependence

The ability to tune the reservoirs, both in a volatile and non-volatile manner is an important feature for the devices, both in terms of short term optimisation and longer term network design. Magnetic vortices have a strong magnetic field dependence, which has been discussed in many previous publications [3,4]. Unfortunately this field dependence is strongly modulated by the impact of the grains in this magnetic materials. The grains, which are typically of the order of the size of the vortex core itself, and cause a significant modification of the energy landscape which results in the magnetic vortex core being pinned in various different local energy minima. This can be seen in Figure 6 where the spin diode voltage for a device with a free layer of 7nm NiFe is shown as a function of the in-plane magnetic field for an excitation current (-20dBm) which is sufficient for the vortex core to remain pinned. The resonance frequency, i.e. where a peak in voltage is observed, varies strongly between 0.1 and 2 GHz as a function of the in-plane field, which can be understood in terms of the vortex core moving between different pinning sites and each pinning site having a different resonant frequency. The first order azimuthal spin wave mode is also visible between 3-5 GHz, and can also be seen to fluctuate with the impact of the grains, however as this mode occurs in the body of the vortex, rather than the core itself, it is less sensitive to the impact of the defects.

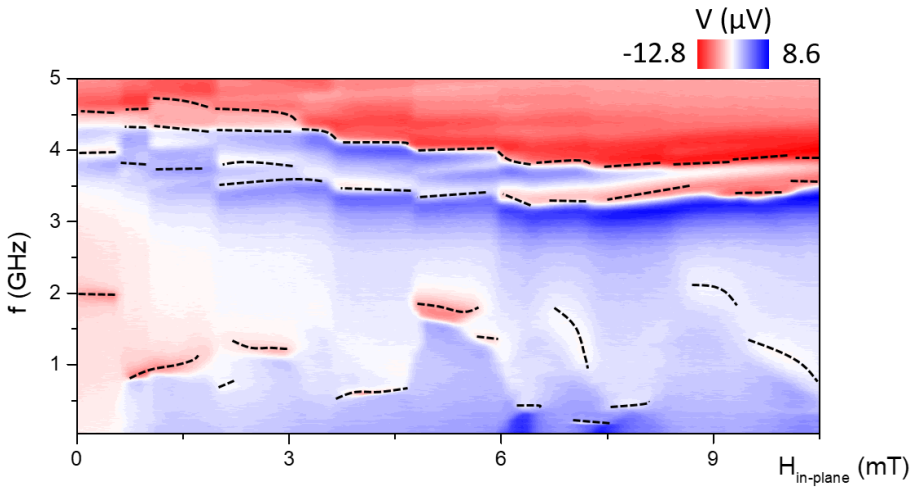


*Figure 7 – in-plane magnetic field dependence of the spin diode voltage of a 1 micron device with a free layer 7nm NiFe.*

The field dependence of the spin diode measurement when the vortex core is excited with low rf powers, and this remains pinned, can be seen in Figure 8. The impact of the grains is significantly less for the amorphous CoFeSiB devices, however it is still noticeable. As this variation of the frequency is unique to each device it represents a significant potential hurdle to overcome for reservoir design.

This project has received funding from the EU Research and Innovation Programme Horizon Europe under grant agreement No 101070290.

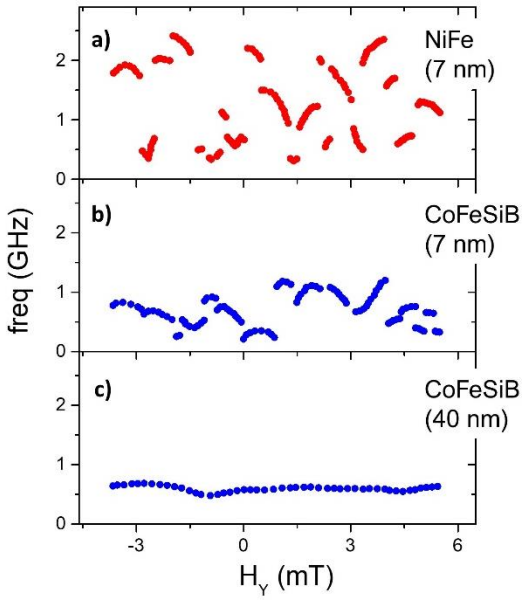


*Figure 8 – in-plane field dependence of the spin diode measurement made at an rf power of -20dBm for three different free layers, i.e. NiFe (7nm), CoFeSiB (7nm) and CoFeSiB (40nm)*

Instead of applying an in-plane magnetic field, which will move the magnetic vortex core from one local pinning site to another, in Figure 9 a perpendicular magnetic field is applied which modifies the magnetic properties without displacing the vortex core. The device under investigation is an 80nm thick CoFeSiB free layer of diameter 1 micron, and a dc current of 16 mA is applied and the resultant thermal spectra is amplified 40dB and measured with a spectrum analyser. The dotted lines have been added to show the evolution of the modes present in the vortex as a function of the perpendicular magnetic field. Both field sweep directions are shown, and a discontinuity can be observed for negative fields when the sweep starts at large positive magnetic fields and positive when the field starts at large negative magnetic fields, corresponding to the reversal of the vortex core polarity. The higher order spin wave modes whose frequency is f>3GHz at zero field tend to all reduce in frequency as a function of the applied magnetic field. The impact of the perpendicular field will be to tilt the magnetisation out of plane and increase the size of the magnetic vortex core. This field dependence can be further explored in WP3.

This project has received funding from the EU Research and Innovation Programme Horizon Europe under grant agreement No 101070290.

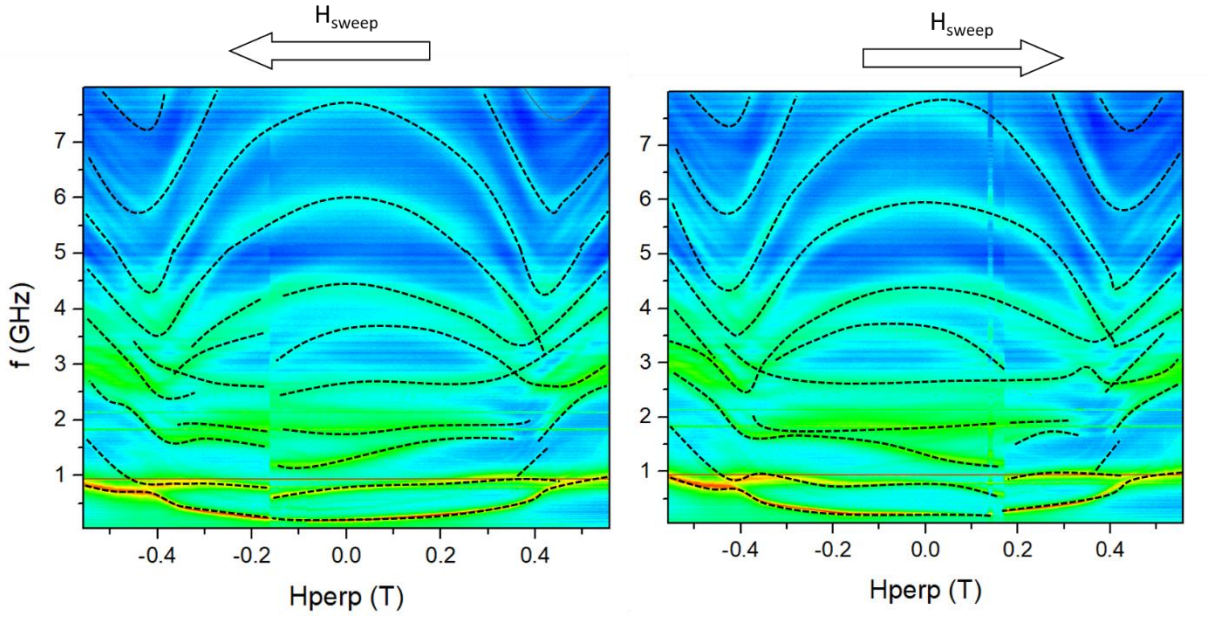


*Figure 9 – FMR measurement of the available modes in a 1 micron pillar with an 80 nm CoFeSiB free layer as a function of an applied perpendicular magnetic field, for the field swept from positive to negative and negative to positive.*

### 3.1.6 MTJ bias dependence

In Figure 9 the concept of non-volatility appears in the form of the vortex core polarity, where both positive and negative core polarities can be stabilised, however the magnetic fields required for the switching of the vortex core are impractical and the variation in dynamic properties between the two polarities is limited. Another feature of the magnetic vortex which can offer non-volatile programming is the vortex chirality. The vortex core chirality can be controlled by applying a strong bias current, whose radial Oested field can then program the sense of circulation of the in-plane magnetisation. An example of this is shown in Figure 10 where the FMR spectra of a 80 nm free layer device of 1 micron is presented as a function of the dc bias applied to the MTJ. At zero bias no signal is visible because the thermally excited FMR signal produced by the MTJ is resistive and therefore needs a current to be applied in order to measure via the spectrum analyser. The bias is shown swept from positive to negative and negative to positive, and again a discontinuity can be seen, in the case corresponding to the switching the vortex chirality.

This project has received funding from the EU Research and Innovation Programme Horizon Europe under grant agreement No 101070290.

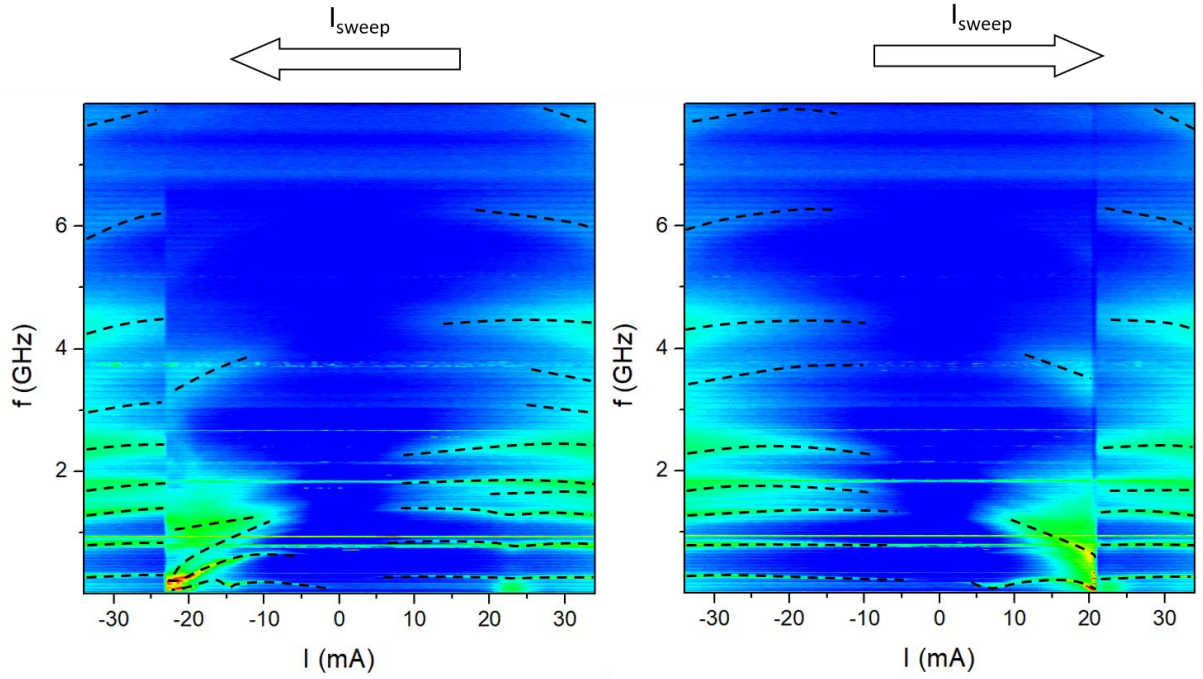


*Figure 10 – bias dependence of the FMR spectra for both bias sweep directions for an 80nm CoFeSiB free layer of diameter 1 micron.*

### 3.1.7 Exciting higher order modes in thick CoFeSiB systems

In Figure 11 an example of the driven dynamics possible in thick MTJ systems is shown, where an rf current of 10dBm is driven across an integrated field line and the resultant spectra in an 80nm thick CoFeSiB free layer of 1 micron diameter MTJ is shown. As the driving frequency ($f_{source}$) is swept is crosses multiple higher order modes, both higher order gyrotropic and spin wave. There is significant scattering from these higher order modes, as demonstrated by the resultant lower frequency peaks.

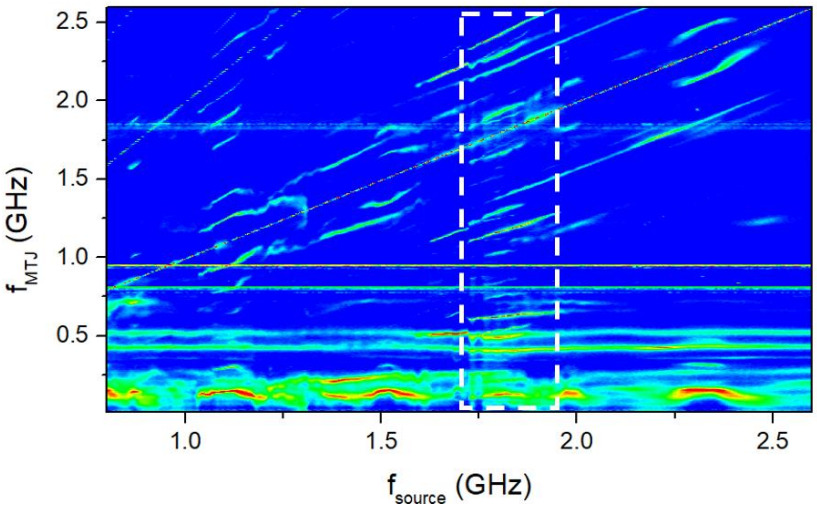


*Figure 11 – example of the driven dynamics in 80nm CoFeSiB 1 micron magnetic tunnel junction, where the rf power measured at the MTJ is plotted as a function of the driving frequency for an input power of 10dBm in the field line antenna.*

This project has received funding from the EU Research and Innovation Programme Horizon Europe under grant agreement No 101070290.

An example of the type of dynamics possible in such complex magnetic systems is shown in Figure 12, where a 1.8 GHz driving signal results in many lower frequency scattering events. The investigation of these extremely complex dynamics is ongoing and will be continued in conjunction with WP3 using simulations.

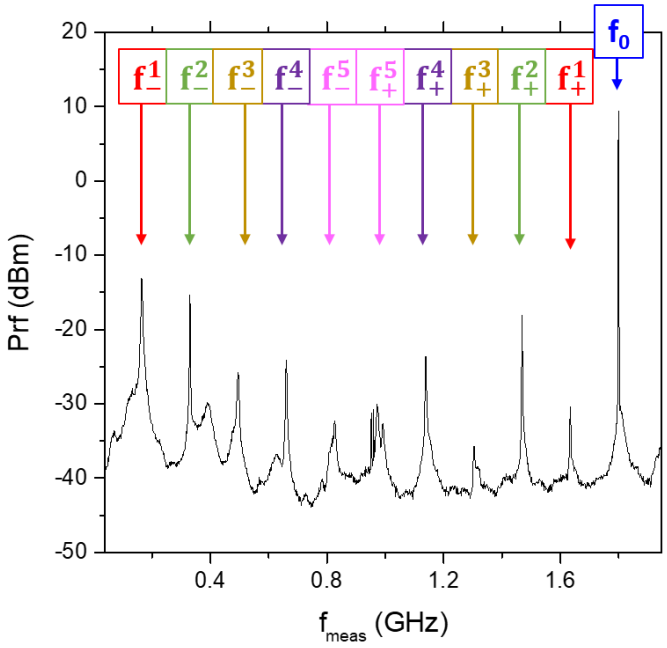


*Figure 12 – example of the complex driven dynamics in 80nm thick CoFeSiB free layer 1 micron MTJ with a driving power of 8dBm.*

## 4 Conclusion and future perspectives

Magnetic tunnel junctions have been fabricated into a range of different diameters and their dynamics have been explored both in terms of their low frequency fundamental gyrotropic mode and the high order spin wave modes. Three dimensional core behaviour has been observed for devices with thickness above 30 nm. This behaviour strongly modifies the dynamics and leads to the emergence of higher order gyrotropic modes which will be explored further in WP3 (Modelling the magnon reservoir in the GHz regime). The complex dynamics in these systems can produce a significant amount of scattering between modes which is necessary for the realisation of the reservoir computing in reciprocal space paradigm. Work will have to continue in conjunction with the WP5 (Electrical readout for wafer-scale integration) and WP6 (Real-world data testing and benchmarking) to assess the optimal mode profile behaviour.

## 5 Bibliography

[1] A. S. Jenkins, L. S. E. Alvarez, S. Memshawy, P. Bortolotti, V. Cros, P. P. Freitas, and R. Ferreira, Electrical characterisation of higher order spin wave modes in vortex-based magnetic tunnel junctions, Commun. Phys. 2021 41 **4**, 1 (2021).

[2] J. Ding, G. N. Kakazei, X. Liu, K. Y. Guslienko, and A. O. Adeyeye, Higher order vortex gyrotropic

This project has received funding from the EU Research and Innovation Programme Horizon Europe under grant agreement No 101070290.

modes in circular ferromagnetic nanodots, 1 (2014).

[3] A. S. Jenkins, E. Grimaldi, P. Bortolotti, R. Lebrun, H. Kubota, K. Yakushiji, A. Fukushima, G. de Loubens, O. Klein, S. Yuasa, and V. Cros, Controlling the chirality and polarity of vortices in magnetic tunnel junctions, Appl. Phys. Lett. **105**, 172403 (2014).

[4] A. Dussaux, A. V Khvalkovskiy, P. Bortolotti, J. Grollier, V. Cros, and A. Fert, Field dependence of spin-transfer-induced vortex dynamics in the nonlinear regime IN THE LINEAR REGIME, **014402**, 1 (2012).

This project has received funding from the EU Research and Innovation Programme Horizon Europe under grant agreement No 101070290.